PERGAMON

Journal of Structural Geology 22 (2000) 669–681

JOURNAL OF STRUCTURAL GEOLOGY

www.elsevier.nl/locate/jstrugeo

The Maxwell stability criterion in pseudo-energy models of kink banding

Giles W. Hunt, Mark A. Peletier [1], M. Ahmer Wadee*, [2]

Department of Mechanical Engineering, University of Bath, Bath BA2 7AY, UK

Received 30 April 1999; accepted 3 December 1999

Abstract

Kink banding, common to many structures in nature and engineering, has several distinctive features—notably highly non-linear snap-back instability leading to localization and sequential lock-up. The proposed friction model, although simplified, introduces these defining characteristics without obscuring them by including other effects of lesser immediate significance. In the absence of small imperfections or disturbances, linearized theory suggests that in its pre-kinked configuration the system never goes unstable. However, under sufficient applied end-displacement it is in a state of extreme metastability, such that micro-disturbances would trigger a non-linear response. This is overcome when an energy approach based on a global rather than a local stability criterion is used. When applied to imperfect systems with small initial misalignments, the critical displacement thus defined shows little of the sensitivity expected from other stability criteria, and provides a lower bound on the expected critical displacement and associated load.

1. Kink bands in layered structures

The phenomenon of kink banding is known throughout the engineering and geophysical sciences. Associated with layered structures compressed in a layer-parallel direction, it arises for example in stratified geological systems under tectonic compression (Price and Cosgrove, 1990), on a micro-scale in wood and fibre composites (Reid and Peng, 1997; Fleck, 1997), and internally in wound ropes (Hobbs et al., 1995). There are several well-known experimental papers on the subject (see for example Paterson and Weiss, 1966; Hobbs et al., 1982; Williams and Price, 1990) but a number number of technical difficulties appear endemic to the modelling of such systems. Continuum formulations based on anisotropic elasticity suffer from a change in character, from elliptic to hyperbolic; consequently projected results tend to be unrealistic (Hobbs et al., 1976, p. 207). Even when Cosserat (couple-stress) continua are used to overcome such problems, the large rotations require a specialized, geometrically non-linear treatment (Fleck et al., 1995; Fleck, 1997; Adhikary and Dyskin, 1997, 1998; Adhikary et al., 1999). Even for the simplest mechanical models, perfect systems tend to exhibit infinite critical loads, with the corollary of extreme sensitivity to small disturbances or geometric misalignments.

We shall concentrate here on the geological manifestation of kink banding, which when seen from a structural mechanics perspective has a number of distinctive features. Simple experiments on stacks of paper (see Figs. 1(a, b) and 2) show an intriguing sequence of phases. The initial instability appears as a *jump phenomenon*: it is so unstable that so-called *snap-back* behaviour is observed where, under conditions of controlled end displacement, the load drops significantly as the system moves suddenly from the flat undeflected state to that of a single

* Corresponding author.
E-mail address: a.wadee@ic.ac.uk (M.A. Wadee).
[1] Current address: Centrum voor Wiskunde en Informatica, P.O. Box 94079, 1090 GB Amsterdam, The Netherlands.
[2] Current address: Department of Civil and Environmental Engineering, Imperial College of Science, Technology and Medicine, Imperial College Road, London SW7 2BU, UK.

0191-8141/00/$ - see front matter
PII: S0191-8141(99)00182-0

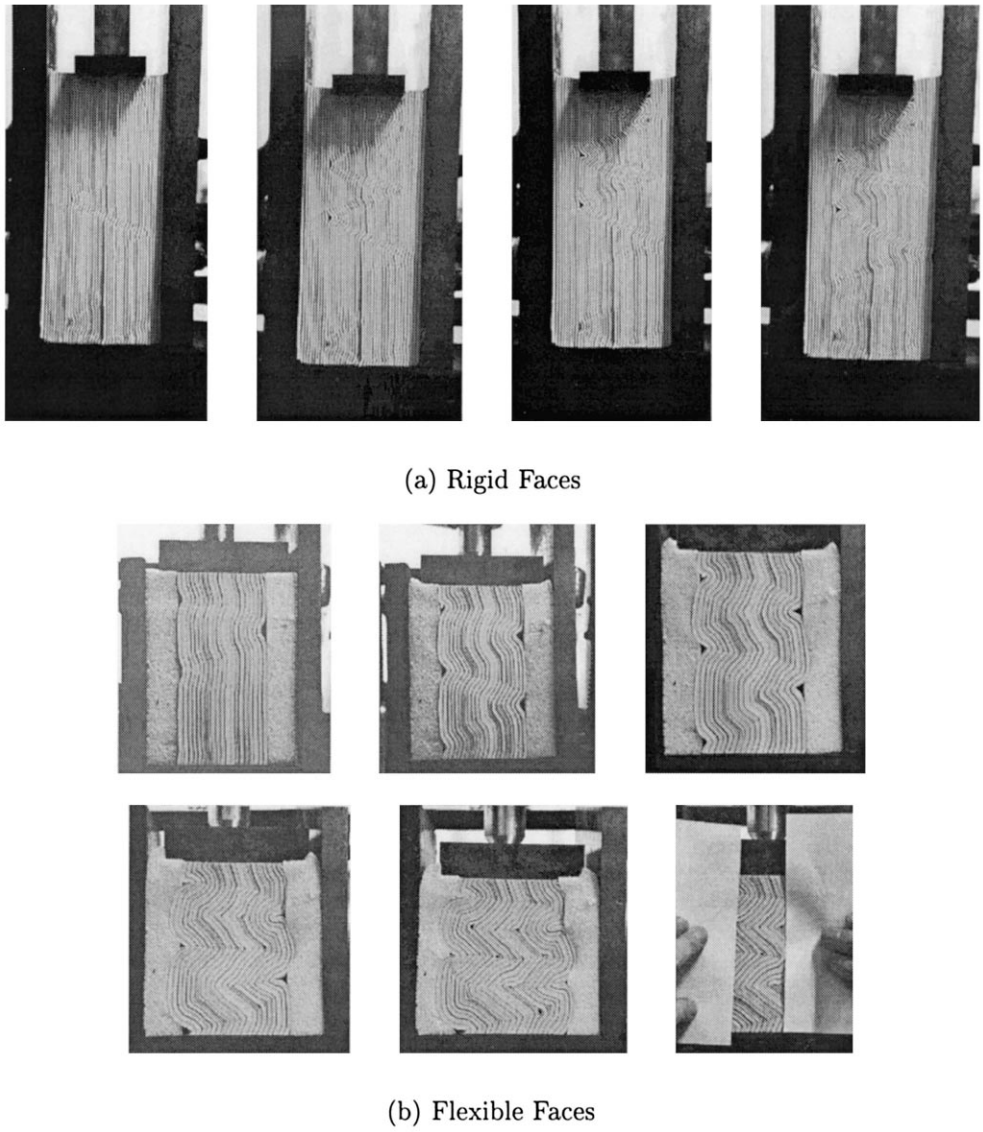

Fig. 1. Compression test on layers of paper restrained between differing faces.

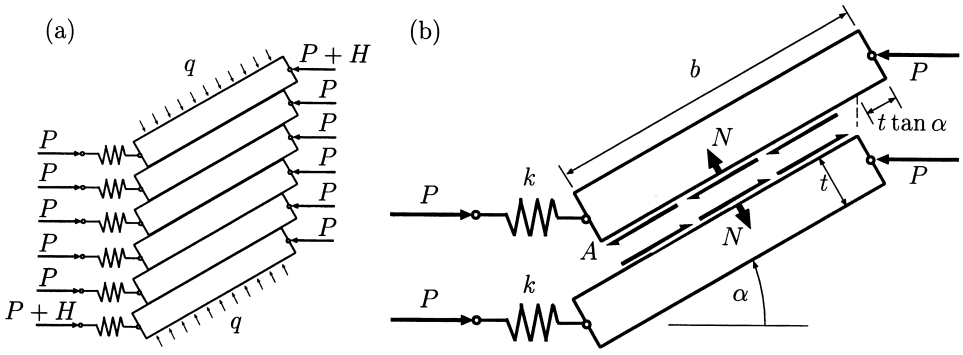

Fig. 2. (a) Full stack of blocks, showing external loading, P, overburden pressure, q, and horizontal reactions, H. (b) Representative two-layer section, K is the stiffness of the inline springs.

kink band involving a large but localized displacement. Yet once the jump has taken place, stability is found in the kinked configuration: the next phase marks a spreading of the bands throughout the specimen, into a periodic pattern with wavelength governed by kink-band angle and specimen width rather than overall length, band width or layer thickness. A final third stage sees transition from a spread of kink bands to overall chevron folding (see Fig. 1b), which inevitably involves the migration of fold lines.

The initial, single kink band clearly represents a highly localized form of deformation, where all lateral deflection is concentrated in a narrow band. Kink banding also shows a second form of localization, in the relative tightness of the hinges seen in Fig. 1(a). Here localization is within the band itself; the deformation is not evenly spread, but concentrated on the boundaries. Experiments, such as those shown in Fig. 1, suggest that this does not occur to the same degree in all kink bands, and seems to be related to confining pressure: the greater the penalty for the formation of voids between the layers, the sharper the hinges. Plastic yielding is often advanced as the explanation for this localization of strain, but in a geological framework, plasticity is neither necessary nor sufficient to explain this.

The object of this paper is to reproduce the early stages of the kink-banding process in a simplified model. To reproduce the jump behaviour observed experimentally, we give the system an initial layer-parallel stiffness that enables elastic unloading into the kinked region. Inter-layer friction is introduced according to a simple Coulomb law. Because of the large rotations, the model is inherently non-linear; indeed it is a central tenet that linearized or small-deflection models bear little or no relation to the final outcome. Also, we adopt an energy or virtual work formulation, and thus side-step the impractical issue of infinite critical loads by adopting the Maxwell criterion of stability (Zeeman, 1977, p. 53) arguing that underlying disturbance is such that buckling is triggered when enough strain energy is stored in the initial precompression to overcome internal work against friction: such a system will always seek a global, as opposed to a local, energy minimum. This criterion is known to be useful when localization and locking-up are part of the picture (Hunt et al., 1999), and is seen here to be robust against initial misalignments.

The simplified friction model is not necessarily quantitatively accurate. Indeed, as the formulation develops we will identify additional energy contributions that could have been included in a more complete development. Thus the friction model is seen merely as one of a generic family, which might eventually be combined in a sophisticated model with predictive qualities. Presently, only the possibility of such extensions is highlighted.

2. Prototype models

2.1. Vertical stacking

Consider the stack of layers of Fig. 2(a). Fig. 2(b) shows a representative two-layer section from the middle of this stack. Each layer is of thickness t, preset length b, and supports a conservative load P. The upper and lower exposed surfaces are subject to a fixed distributed normal load q, representing the overburden pressure. Layer-parallel stiffness is represented by inline springs of stiffness k. Horizontal reaction forces H are introduced top and bottom to maintain equilibrium. For ease of description the layers are aligned vertically, although in practice they would be inclined (see Section 2.2). No energy terms are included to represent work done at the sharp hinges or folds, and to compensate, the kink bandwidth b is fixed a priori. Bending energy in the hinges is expected to be significant in determining the true value of b, as discussed later. This formulation allows the introduction of non-linear behaviour in a succinct manner.

The equilibrium equations for this system are derived by minimizing a total potential energy function, constructed by adding separate potentials for each of the components. Although friction is not conservative, we assume that layers slide in the same direction throughout the deformation process; this justifies a pseudo-energy description of the work done by friction and mimics a conservative process.

The interlayer forces are assumed to sum to a normal force N and a friction force A. Assuming a Coulomb friction law, A satisfies $0 \le A \le \mu N$, where μ is the coefficient of friction. However, A could conceivably take other forms. For example, if A is taken constant, the response would have much in common with the plastic shear model of Budiansky et al. (1998).

Vertical equilibrium condition for the top block in Fig. 2(a) gives,

$$qb \cos \alpha = N \cos \alpha - A \sin \alpha. \tag{1}$$

If A is assumed to be always at the critical state $A = \mu N$, we can single out N,

$$N = \frac{qb}{1 - \mu \tan \alpha}. \tag{2}$$

Note that N is only positive if $\alpha < \operatorname{arccot} \mu$. Using moment equilibrium for a typical middle block,

$$P = \frac{Nt(\tan\alpha + \mu)}{b \sin\alpha} = \left(\frac{qt}{\sin\alpha}\right)\left(\frac{\mu + \tan\alpha}{1 - \mu\tan\alpha}\right). \tag{3}$$

The work done by the friction force is then

$$\begin{aligned} W_{\mathrm{Fr}} &= -\int_0^{\alpha} \mu N(\alpha')\, \mathrm{d}(t\tan\alpha') \\ &= -\int_0^{\alpha} \frac{qb\mu}{1 - \mu\tan\alpha'} \mathrm{d}(t\tan\alpha') \\ &= -\mu qbt \int_0^{\alpha} \frac{\sec^2\alpha'}{1 - \mu\tan\alpha'} \mathrm{d}\alpha' \\ &= qbt\ln(1 - \mu\tan\alpha), \end{aligned} \tag{4}$$

provided $\alpha < \operatorname{arccot}\mu$. Since the layers slide in the same direction throughout the deformation, we can interpret this work as a pseudo-energy,

$$V_{\mathrm{Fr}} = -W_{\mathrm{Fr}}. \tag{5}$$

From this energy term we subtract the work done by the point forces P and the distributed force q (Fig. 2):

$$W_{\mathrm{P}} = Pb(1 - \cos\alpha) \tag{6}$$

$$\begin{aligned} W_{\mathrm{q}} &= -\int_0^{\alpha} qb\cos\alpha'\, \mathrm{d}(t/\cos\alpha') = -qbt\int_0^{\alpha} \tan\alpha'\, \mathrm{d}\alpha' \\ &= qbt\ln\cos\alpha, \end{aligned} \tag{7}$$

and we add the potential associated with the compression δ of the springs k,

$$V_k = \frac{1}{2}k\delta^2 - P\delta. \tag{8}$$

This yields the total potential energy

$$\begin{aligned} V = V_k + V_{\mathrm{Fr}} - (W_{\mathrm{P}} + W_{\mathrm{q}}) &= \frac{1}{2}k\delta^2 \\ - qbt\ln(\cos\alpha - \mu\sin\alpha) &- P[\delta + b(1 - \cos\alpha)]. \end{aligned} \tag{9}$$

At this point we replace P, a point force, by p, a distributed force, which are related by $P = pt$. This makes p commensurate with q and will be more convenient for later models. In addition, we non-dimensionalize the problem by considering t as a typical length scale and k as a measure of force per unit area. Setting

$$\delta = t\tilde{\delta}, \quad b = t\tilde{b}, \quad q = k\tilde{q}, \quad p = k\tilde{p}, \tag{10}$$

and dropping the tildes immediately, the non-dimensionalized potential energy is

$$V = \frac{1}{2}\delta^2 - qb\ln(\cos\alpha - \mu\sin\alpha) - p[\delta + b(1 - \cos\alpha)]. \tag{11}$$

Stationary points of this energy satisfy the two equilibrium equations

$$p = \delta \tag{12}$$

$$p = \frac{q}{\sin\alpha}\frac{\mu + \tan\alpha}{1 - \mu\tan\alpha}. \tag{13}$$

The interesting curve to plot is that of p against Δ, the total end-shortening given by

$$\Delta = \delta + b(1 - \cos\alpha). \tag{14}$$

By parameterizing in α, the variation of p with end-shortening Δ over a range of different but constant q values is as shown in Fig. 3. Each curve approaches both the flat state $\alpha = 0$ and the locked-up state $\alpha = \operatorname{arccot}\mu$ asymptotically as $p \to \infty$. The curves imply among other things the absence of critical bifurcation loads for $q \neq 0$ over the full range of finite p.

2.2. Inclined geometry

Actual kink bands do not form orthogonal to the layering. A simple explanation is that the increase in height ($t \longmapsto t/\cos\alpha$) occupied by a layer in the vertical stack forces the adjoining layers apart; the voids thus created represent significant work against the overburden pressure. A more realistic mode of deformation is shown in the stylized geometry of Fig. 4. As the angle α increases, the angle β of the band also increases, and provided that α remains equal to 2β throughout the deformation the layer distance is the same in the kink band as in the unbuckled layers.

The inclined geometry leads to two changes in the model outlined in the previous sections. First, the distance that two layers slide with respect to each other is now $t\tan(\alpha - \beta) = t\tan\alpha/2$. For this geometry the fric-

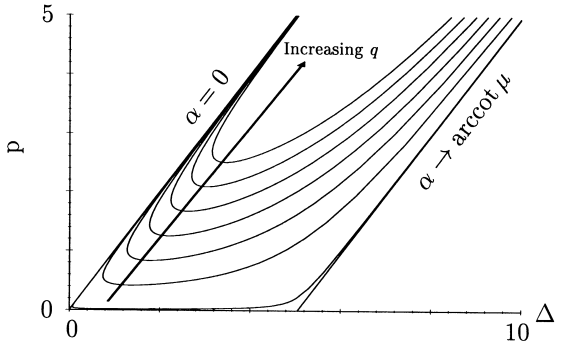

Fig. 3. Equilibrium solutions on a plot of load p against total end-shortening Δ for varying q with constants $\mu = 0.57$ and $b = 10$.

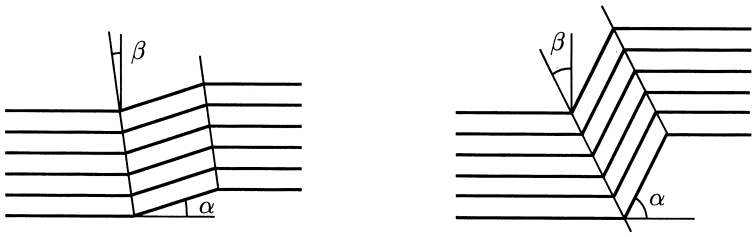

Fig. 4. The inclined stack. For the distance between folding layers to remain constant, the kink band angle β must vary according to $\alpha = 2\beta$.

tion 'energy' becomes, in non-dimensionalized form,

$$V_{\mathrm{Fr}} = -W_{\mathrm{Fr}} = \int_0^{\alpha} \mu N(\alpha')\, \mathrm{d}(\tan \alpha'/2)$$

$$= \frac{\mu q b}{2} \int_0^{\alpha} \frac{\sec^2(\alpha'/2)\, \mathrm{d}\alpha'}{(1 - \mu \tan \alpha')}. \tag{15}$$

Although this integral has an explicit solution, we leave it as it stands for brevity. Secondly, the work done by p and against q needs to be recalculated. The total work done by these external forces was determined as $pb(1 - \cos \alpha) + qb \log \cos \alpha$ in the original, vertical, stack of layers. For convenience we split p into two parts, $p = p_1 + q$, such that p_1 is the layer-parallel applied load that is additional to q. Since $\alpha = 2\beta$ the deformation is volume-conserving and thus q does no work (see Fig. 5). Note that if the condition $\alpha = 2\beta$ is relaxed, and β is allowed to take values larger than $\alpha/2$, the volume is not conserved—the layers inside the kink band separate (dilatation) resulting in the release of friction and the introduction of an extra component of work done against overburden pressure q. Owing to this, voids quickly diminish and the region returns to its original volume ($\alpha = 2\beta$), contact reintroduces frictional forces and the response returns to that of the above model. We intend to cover dilatation in future work.

The non-dimensionalized total work done by p and q per single layer is therefore equal to $W_{\mathrm{p}} + W_{\mathrm{q}} = p_1 b(1 - \cos \alpha) = (p - q)b(1 - \cos \alpha)$. In the tilting geometry the energy thus becomes,

$$V = \frac{1}{2}\delta^2 - p\delta + \frac{\mu q b}{2} \int_0^{\alpha} \frac{\sec^2(\alpha'/2)\, \mathrm{d}\alpha'}{(1 - \mu \tan \alpha')}$$

$$- (p - q)b(1 - \cos \alpha) \tag{16}$$

and the equilibrium equations are

$$p = \delta$$

$$\frac{p}{q} = 1 + \frac{\mu}{\sin \alpha(1 + \cos \alpha)(1 - \mu \tan \alpha)}. \tag{17}$$

Fig. 6 shows the equilibrium curves of both the vertical and the inclined kink bands. Because the layers slide less in the inclined geometry ($\tan \alpha/2$ instead of $\tan \alpha$) the friction energy is less, leading to a smaller total strain energy.

3. Maxwell stability criterion

Starting from the undeflected state, varying either load p or end-displacement Δ would cause the system to move up the straight line in Fig. 3. As all equilibria on this path are local energy minima, according to the standard delay stability conven-

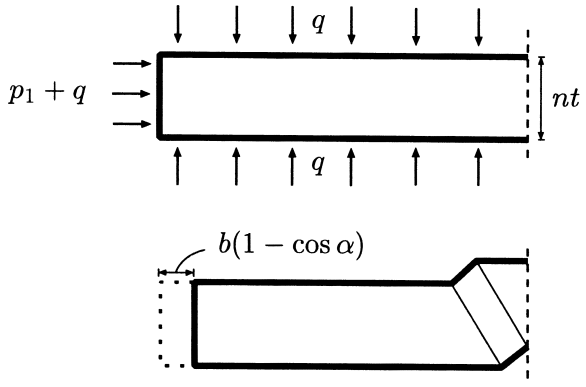

Fig. 5. Work done by the pressures p and q during the inclined-geometry deformation. The stack contains n layers, and the dashed vertical line denotes an axis of symmetry.

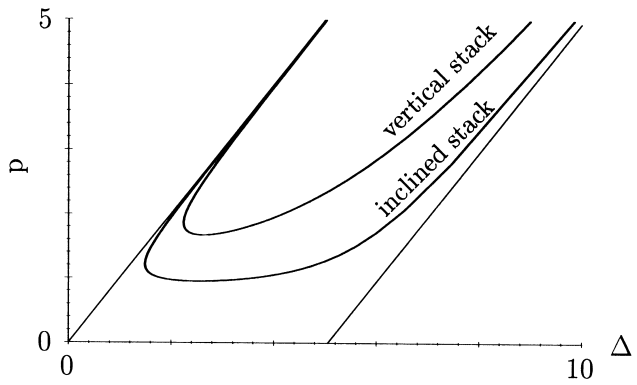

Fig. 6. Equilibrium curves for the straight and for the inclined geometry. Here $q = 0.5$, $\mu = 0.57$, and $b = 10$.

tion—which can be described as 'stay in an equilibrium state as long as it is a local energy minimum; move when this fails'—the critical load is infinite. However, high loads imply an extreme state of metastability, as the slightest disturbance would trigger the jump response. In this situation, linear eigenvalue and perturbation analyses are of little use, as they provide no mechanism for jumping the gap between the equilibrium solutions. They must be replaced by a non-linear method geared to stability in the presence of disturbances. As such a system may respond differently depending on whether the load or end-displacement is controlled, the loading conditions first need to be carefully specified.

Here we assume rigid loading conditions such that end-shortening Δ is the controlled parameter (Thompson and Hunt, 1973). To cover the problem of infinite critical loads we adopt the so-called *Maxwell stability criterion* (Zeeman, 1977, p. 53; see also Biot, 1965, p. 204 for an early mention in the geological context) where stability rests only with the global, as opposed to any local, minimum of total potential energy. The Maxwell law is commonly used for thermodynamical instability, for instance in modelling phase transitions where underlying disturbances and statistical fluctuations ensure that the system shakes out of local minima and seeks a global energy minimum. The same criterion has recently been applied to a number of structural problems with the destabilizing/restabilizing (localizing/locking-up) characteristics as found here (Hunt et al., 1999).

Consider for the moment a typical load/end-shortening response graph for an elastic structure, which twice bends back on itself, as shown schematically in Fig. 7. If Δ is the controlled parameter, the area under the graph represents the strain energy stored. Over a certain range of Δ the response is triple-valued. Of the three possible candidates for equilibrium, **A** and **C** are local energy minima and **B** is a local maximum.

Stored strain energies at **A**, **B** and **C** are as shown; area A_1 represents the energy hump to be overcome in moving from **A** to **B**, while area A_2 is energy that is available for release in moving from **B** to **C**. For the 'delay' stability convention the system may remain at either **A** or **C**, while under the Maxwell criterion, stability rests only with state of lower energy. The *Maxwell displacement* Δ_M is the value of end-shortening where the minimum swaps from **A** to **C**, and hence $A_1 = A_2$.

The Maxwell criterion seems apt when applied to a system with a localized response like that of Fig. 3. A_1 is now the work done against friction; it continues to $p = \infty$ yet is very thin—more of an energy spike than energy hump—and by nature would be extremely sensitive to imperfections. Moreover, the more severe the localization, the sharper the spike. A_2 is the energy available from the pre-compression, and is of a generally more robust shape. The net effect is that a slight increase in Δ from the Maxwell position will change A_1 only a little, but enlarge A_2 considerably. Thus not only is the spike easily eroded by imperfections, but the stored energy available for release is significantly enhanced by only a small change in Δ. The Maxwell displacement thus provides a robust lower bound to the actual critical displacement for kink banding.

We will now calculate the value of Δ_M and the associated value α_M for both the vertical and the inclined stack. Fig. 8(a) shows the situation in caricature. Note that $p \to \infty$ as $\alpha \to 0$ on the upper, and similarly $p \to \infty$ as $\alpha \to \operatorname{arccot} \mu$ on the lower, branch of the curve in Fig. 3. On integrating from $\alpha = 0$ to the value $\alpha = \alpha_M$, the area of interest, shaded in Fig. 7, is given by

$$\text{Area} = \int_{\alpha=0}^{\alpha=\alpha_M} (p - \Delta)\, \mathrm{d}\Delta. \tag{18}$$

3.1. Vertical stack

Differentiation of Eq. (14) gives $\mathrm{d}\Delta = \mathrm{d}\delta + b \sin\alpha\, \mathrm{d}\alpha$, and after substituting the equilibrium Eqs. (12) and (13) this integral can be written,

$$\text{Area} = -\frac{1}{2}\Delta^2\Big|_0^{\alpha_M} + \frac{1}{2}\delta^2\Big|_0^{\alpha_M} + qb \ln(\cos\alpha - \mu \sin\alpha)\Big|_0^{\alpha_M}. \tag{19}$$

If it is zero, the Maxwell condition is satisfied for a jump from the upper straight line representing the

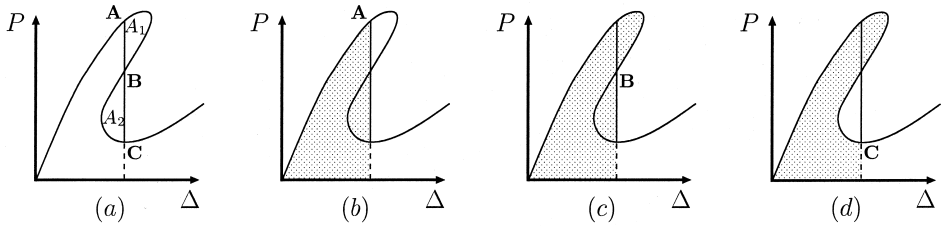

Fig. 7. Strain energy under controlled end-shortening Δ. (a) Three possible equilibrium states **A**, **B**, and **C**. (b) Strain energy at **A**. (c) Strain energy at **B**. (d) Strain energy at **C**.

undeflected state, to the lower branch of the curve. Substituting for Δ, δ, and p in terms of α then leaves the equation

$$\ln(\cos\alpha_M - \mu\sin\alpha_M) - \frac{(1-\cos\alpha_M)(\sin\alpha_M + \mu\cos\alpha_M)}{\sin\alpha_M(\cos\alpha_M - \mu\sin\alpha_M)} = \frac{b}{2q}(1-\cos\alpha_M)^2, \quad (20)$$

from which the particular Maxwell displacement Δ_M can be found, where energy levels in pre-buckled ($\alpha = 0$) and post-buckled ($\alpha = \alpha_M$) states match. Fig. 8 shows the values of Δ_M for two different values of q.

3.2. Inclined stack

Similarly, for the inclined stack, Eq. (18) can be written as

$$\text{Area} = -\frac{1}{2}\Delta^2\Big|_0^{\alpha_M} + \frac{1}{2}\delta^2\Big|_0^{\alpha_M} + qb\left[\int_0^{\alpha_M}\frac{\mu\sec^2(\alpha/2)\,d\alpha}{2(1-\mu\tan\alpha)} + (1-\cos\alpha)\Big|_0^{\alpha_M}\right] \quad (21)$$

and substituting for δ, Δ, and p, gives the following equation at the Maxwell displacement ($\alpha = \alpha_M$):

$$\int_0^{\alpha_M}\frac{\mu\sec^2(\alpha/2)\,d\alpha}{2(1-\mu\tan\alpha)} - \frac{1-\cos\alpha_M}{\sin\alpha_M(1+\cos\alpha_M)(1-\mu\tan\alpha_M)} = \frac{b}{2q}(1-\cos\alpha_M)^2, \quad (22)$$

with Fig. 8(c) showing Δ_M for two different values of q.

4. Impact of imperfections

In reality, the infinite critical load of the perfect system is not expected to survive the introduction of misalignments or other small imperfections. As we see below the infinite spike is lost, and we witness the appearance of a 'peak load' at which the unbuckled state loses local stability. The level of this peak load depends strongly on the magnitude of the imperfections. As a result, a large body of research has developed into the impact of imperfections on the peak load. (For an overview in the field of fibre-reinforced composites, see Fleck, 1997.)

Part of our interest in the Maxwell criterion is motivated by the fact that the critical displacement given by this criterion, and the corresponding load at this displacement, are much less sensitive to the size of the imperfections than is the peak load. In the example that we study below this becomes clear.

4.1. Initial misalignment

As an example of an imperfection we commence loading at a small initial misalignment, i.e. we start

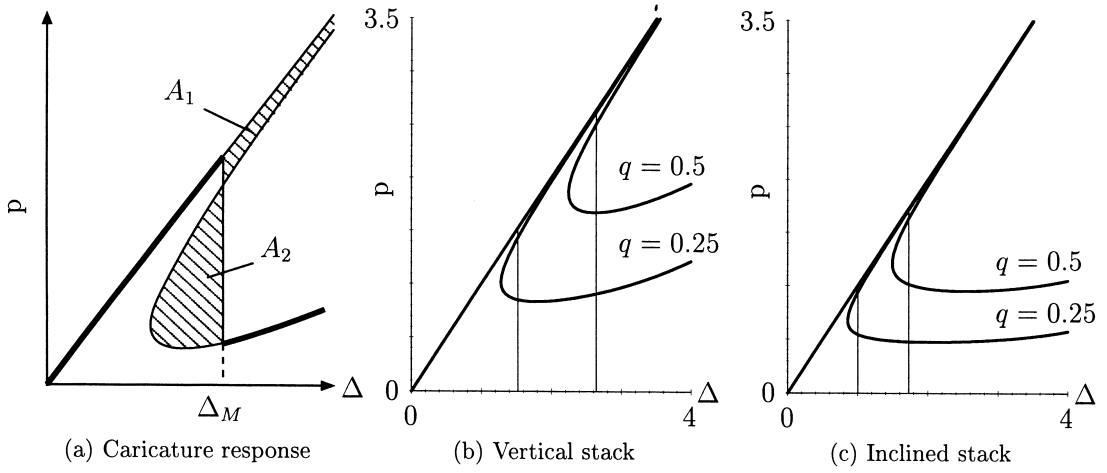

Fig. 8. Equilibrium solutions on a plot of load p against total end-shortening Δ. Thin vertical lines mark positions of the Maxwell displacement Δ_M.

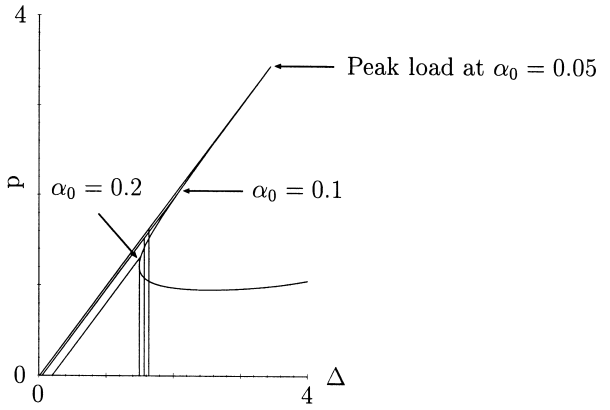

Fig. 9. Variations of peak load and Maxwell displacement with initial misalignments. Here $\mu = 0.57$ and $q = 0.5$.

with $\alpha = \alpha_0 > 0$. Instead of rounding off the gap between the paths, as would be expected for more general forms of imperfection (see for example Golubitsky and Schaeffer, 1984), in this case it acts merely to shift horizontally the unbuckled path, such that it then intersects the curve of the buckled path. Fig. 9 shows the load–deflection diagram for three different non-zero values of α_0. Observe the wide variation in the peak load with different values of α_0, and the corresponding narrow variation of Maxwell displacement Δ_M, and associated load p_M, as shown in Table 1. We conclude that the imperfection removes only a small amount of energy from the total energy hump that needs to be overcome by outside disturbances.

5. Comments on the modelling

From a model as simplified as the one above one should not necessarily expect realistic quantitative results. It is constructed with two purposes in mind:

1. To demonstrate the application of the Maxwell criterion to imperfection-sensitive snap-back phenomena such as kink banding;
2. To help select the most significant modelling characteristics of the kink-band phenomenon from amongst all possible competing alternatives.

Table 1
Comparison of imperfect peak loads p_{peak} against Maxwell displacements Δ_M and corresponding loads p_M

α_0	p_{peak}	Δ_M	p_M
0	∞	1.726	1.726
0.05	3.437	1.637	1.625
0.1	2.018	1.570	1.520
0.2	1.319	1.499	1.300

5.1. The Maxwell criterion

The Maxwell criterion is normally applied where load rather than displacement is the controlled parameter, although Budiansky et al. (1998) used it in the related context of the *broadening* of kink bands. When displacement is controlled and disturbances are rife—folding of geological strata being an excellent example—the Maxwell criterion should provide a realistic and robust lower bound on the actual end-shortening displacement at the first instability. It is however necessary to draw a distinction between the roles of external disturbance and inherent imperfections. While imperfections are local destabilizing factors, in the elastic setting of the pre-compression external disturbances are more likely to appear on the scale of the overall structural dimension. Their effect might therefore be expected to depend on sample length. Adding the fact that long samples have more severe snap-back characteristics than short ones, we can speculate that Maxwell predictions would be most successful when structures are long and failures are local.

To illustrate this, let us assess the strength of a layered structure as studied in this paper. For the moment we assume that we know the structure in detail, including any initial misalignments, but that it is exposed to unknown external disturbances. Suppose it moves, under controlled shortening, along the unbuckled path, until a buckle is triggered. It is reasonable that the peak load is an upper bound of the strength, since disturbances will cause the system to buckle before the peak load is reached. Conversely, the Maxwell load is a reasonable lower bound for the strength, since below this value, a positive energy input from the disturbance is necessary to bring the system to the deflected state.

Moving to a more realistic setting where the magnitude of the misalignment is not known, when peak and Maxwell loads are compared for different misalignments, we observe that the variation is much larger in the former. The Maxwell load should thus provide a more robust starting point for estimations of strength than the peak load.

5.2. The relative importance of assumptions for kink banding

The model discussed here contains three basic ingredients: the inline springs, friction between the layers, and the external forces p and q. We have left out (other) elastic, viscous, and plastic properties, the influence of pore fluid, and many other factors. In addition we assume a highly simplified, although non-linear, geometry that, if interpreted strictly, implies that hinge lines migrate. All these assumptions are clearly incor-

rect for actual materials, but they allow us to make one clear statement, which is subsequently discussed:

> The essence of kink-band formation is captured by layer-parallel stiffness, interlayer friction, and overburden pressure.

1. Layer-parallel stiffness. Both experimental and numerical evidence indicates that the formation of kink bands is a jump phenomenon, in which previously stored energy is released. The layer-parallel stiffness provides this storage.

2. Interlayer friction. As the layers rotate, the lever arm of the moment associated with p increases. For the folds to lock up, a counteracting force is necessary. Friction fulfils this necessity; there is—reasonably—only one alternative in this role, in the form of a deflection-dependent overburden pressure q. However, in the presence of q we would still expect friction to dominate the lock-up state and so it is sensible, at least initially, to involve only the latter.

3. Overburden pressure. The pressure q does however play an important background role. First, a strong overburden pressure in relation to the bending energy of the layers yields folds with straight limbs and tight hinges (see the Appendix). Without overburden pressure, folds would tend to loosen and become rounded, creating voids between the layers. Also, any work done during hinge migration will be small by comparison. Secondly, the overburden pressure acts as a measure for p, in the sense that in Eq. (17) p appears in the combination p/q. For the behaviour of the stack—as opposed to the inline springs—it is therefore not the magnitude of p that is important, but its value relative to q.

While we have shown that the combination of these three elements provides a convincing structure, one might still wonder whether adding on additional elements or assumptions, or relaxing some of the present hypotheses, would in some way improve the model—suggestions are discussed below.

1. Bending energy and plastic hinges. Although the tight-hinge geometry is based on the assumption that the bending energy is dwarfed by the overburden pressure, one might still imagine adding a bending energy (either of elastic or of plastic type) to the potential V in Eqs. (9) or (16). To take the inclined stack model as an example, if we add to V the term $K\alpha^2/2$—for an elastic hinge—this leads to the equilibrium equation

$$\frac{p}{q} = 1 + \frac{\mu}{\sin\alpha(1+\cos\alpha)(1-\mu\tan\alpha)} + \frac{K}{bt}\frac{\alpha}{\sin\alpha}. \qquad (23)$$

Although the numerical value of p is slightly altered by this addition, the main characteristic of the equilibrium curve—p becomes large as $\alpha\to 0$ and as $\alpha\to\operatorname{arccot}\mu$—remains completely unaltered. Consequently the adding of such a term has only a numerical influence on the model, without changing its character. It may however play an important role in determining the value of b.

The same is true for an additional term of the form $K\alpha$, representing the pseudo-energy associated with a plastic hinge. This results in the equilibrium equation

$$\frac{p}{q} = 1 + \frac{\mu}{\sin\alpha(1+\cos\alpha)(1-\mu\tan\alpha)} + \frac{K}{bt\sin\alpha}. \qquad (24)$$

The new term is now singular at $\alpha = 0$, but again the overall character of the equilibrium curves has not changed.

2. Embedding energy. In a similar vein, elastic or plastic embedding energy could be introduced as an alternative to overburden pressure. Whereas the constant pressure of a plastic foundation could be seen as similar in nature to q, the elastic setting would generate terms of a different kind. Questions of whether Winkler (Kerr, 1964) or other foundation assumptions would be appropriate are also relevant, but are left unaddressed at this stage.

3. Hinge migration. In folded geological structures tight hinges can develop secondary deformation structures (e.g. tension gashes in the outer arc). If hinges slowly migrate before reaching their final position, one would expect to find these secondary structures not only in the final position but also along the migration path. The lack of such features in observed strata is sometimes mentioned as an objection to hinge migration.

For the model considered in this paper the paradoxical situation arises that, although in the derivation of the model the hinges migrate over substantial distances, in fact they never actually do. This is related to the concept of the Maxwell criterion, and is illustrated in Fig. 8(a). The thick line and the thin line together represent all equilibrium configurations on the basis of which the Maxwell displacement Δ_M is determined. In an actual system, we expect that under controlled end-shortening Δ the system follows the thick line. For instance, starting from zero displacement, we move up the straight line; at the Maxwell displacement the system *jumps* to the point on the thick curve below and continues up this curve. In this jump, which in practice happens very quickly, the configuration changes from no buckling ($\alpha = \beta = 0$), to $\alpha = \alpha_M$, with $\beta = \beta_M = \alpha_M/2$, implying that, in fact, conceptual hinge migration happens in a jump—instantly at the Maxwell value.

6. Conclusions

The phenomenon of kink banding is seen in many physical systems. In this paper we present a model for stratified geological systems, based on pseudo-energy, accounting for the interlayer friction and the presence of overburden pressure. The pseudo-energy approach mimics a conservative system, which conveniently allows the implementation of the Maxwell stability criterion. This gives insight into the structural behaviour and in its potential to gain quantitative information; in the perfect case the physical model exhibits an infinite critical load, but the Maxwell criterion gives a finite value for the system to jump from an unbuckled to buckled shape at equal energies.

Initial imperfections introduce a finite peak load and reflect an upper bound on the behaviour. Applying the Maxwell criterion to the imperfect model gives a lower bound to the load at which the system loses stability. This lower bound seems to be much less sensitive to the magnitude of the initial imperfection than the peak load. The modelling has been done in a modular way so that, as far as possible, extra effects can be added later. Work is now proceeding to obtain quantitative results in of the kink-banding phenomenon in the laboratory. Preliminary comparisons of Maxwell load levels at the point of instability and kink-band width between experiment and a refined model are encouraging.

Acknowledgements

This work was inspired during a field trip to Cornwall involving geologist, engineers and mathematicians. We would like to acknowledge the following, without whom it would never have taken place. Bruce Hobbs and Alison Ord, Division of Exploration and Mining, CSIRO Perth, Australia, for their introduction to the problem and geological insight, Steve Henley of Resources Computing International Limited in Matlock, UK, for organizing a significant interdisciplinary experience, Ray Lawther, School of Civil Engineering, University of New South Wales, for his help during the modelling process. The work was supported by the EPSRC, through grant GR/L17177 of the Applied Nonlinear Mathematics Initiative.

Appendix. Straight limbs, sharp hinges

An important aspect of the modelling of the preceding sections is the assumption that layers fold in isolated hinges, separated by straight limbs. This is not obvious from the properties of elastic materials, since elastic deformation tends to spread rather than concentrate. The straight-limb, sharp-corner assumption therefore needs justification.

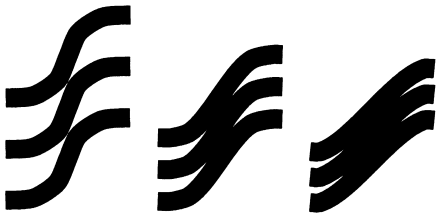

Fig. A1. Sharp-angle, straight-limb folds create fewer voids than rounded folds.

Fold creation in rocks occurs at high confining pressure. Similarly experiments with analogue materials show that a relatively high confining pressure is necessary for the appearance of kink bands. This confining pressure apparently forces the elastic layers to concentrate the deformation into sharp hinges. For a given hinge angle the hinge region has a finite size

$$S_h = \sigma_h \sqrt{EI/PH}, \tag{A1}$$

where σ_h is a constant that only depends on the hinge angle and is independent of all material parameters. Eq. (A1) shows that when the thickness H and the elastic properties EI of the layers are kept constant, the hinge size is a decreasing function of the overburden pressure P. For high overburden pressures we therefore expect to see the hinges localized into sharp corners, connected by straight limbs.

Fig. A1 shows that if a stack of incompressible layers is to fold into a similar fold, then by simple geometry voids are created at the hinges. These voids are costly, in an energy sense, since they represent work done against the overburden pressure. The amount of void created is very sensitive to the form of the fold, as is shown by Fig. A1. Sinusoidal folds create a large amount of void between the layers, while chevron folds are much less costly. This simple, geometric argument shows how a high overburden pressure, which determines the 'unit cost' of void space, can force the

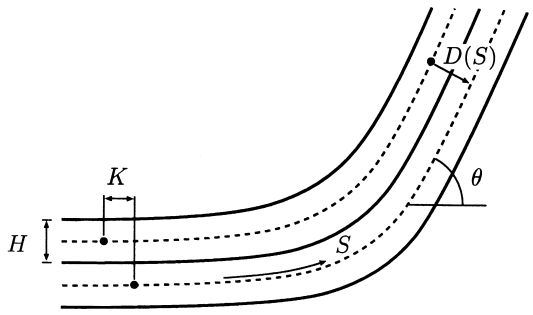

Fig. A2. Two layers in a structure folded into a hinge. The centrelines are indicated by dashed lines.

layers away from the smooth sinusoid folds into sharp-cornered chevron-type patterns.

The model we derive here is inspired by this observation. Consider a structure consisting of identical thin elastic layers, deformed into a single hinge as in Fig. A2. We suppose that the centrelines of the layers are identical copies of each other, each translated by $(K, -H)$ with respect to the layer above, creating a similar-fold hinge. Choosing S as the arclength coordinate, we represent the centreline by the angle $\theta = \theta(S)$ with the horizontal.

If the layers are long with respect to the hinge zone the fold can be modelled by unbounded layers, with $\theta \to 0$ as $S \to -\infty$ and $S \to \theta_\infty$ as $S \to \infty$. We also suppose that for large $|S|$ the centrelines are separated by their 'natural' distance H; this implies that $\theta_\infty = 2\arctan(K/H)$, so that the choice of the hinge angle fixes the value of K and vice versa. (Note that capitals indicate dimensional quantities and lower case indicate their dimensionless equivalents.)

We characterize the optimal configuration as the minimizer of an appropriate energy. With this argument in mind the two elements that we believe to be important are the bending energy of the individual layers and the penalization of voids owing to the overburden pressure. The bending energy can be modelled by

$$\frac{EI}{2}\int_{-\infty}^{\infty} \theta'(S)^2 \, \mathrm{d}S; \tag{A2}$$

for the penalization of voids we need to make some approximations.

Let $D(S)$ be the distance between the centreline of the layer at the point S and the layer below it (Fig. A2). Writing $(X(S), Y(S))$ for the coordinates of the centreline at S, the distance can be characterized as

$$D(S)^2 = \min_{T\in\mathbb{R}} \left|(X(S), Y(S)) - (X(T) + K, Y(T) - H)\right|^2. \tag{A3}$$

At the value of T where this minimum is attained, we have

$$(X(S) - X(T) - K, Y(S) - Y(T) + H) \cdot \frac{\mathrm{d}}{\mathrm{d}T}(X(T), Y(T)) = 0. \tag{A4}$$

Using $X'(T) = \cos\theta(T)$, $Y(T) = \sin\theta(T)$, this implies

$$(X(S) - X(T) - K)\cos\theta(T) + (Y(S) - Y(T) + H)\sin\theta(T) = 0. \tag{A5}$$

Next we make the assumption that θ varies gradually along the layer, so that $X(S) - X(T) \approx (S - T)\cos\theta(T)$ and $Y(S) - Y(T) \approx (S - T)\sin\theta(T)$. Then Eq. (A2) becomes

$$(S - T) - K\cos\theta(T) + H\sin\theta(T) \approx 0. \tag{A6}$$

We can then write

$$\begin{aligned} D(S)^2 &= (X(S) - X(T) - K)^2 + (Y(S) - Y(T) + H)^2 \\ &\approx (X(S) - X(T) - K)(S - T)\cos\theta(T) \\ &\quad + (Y(S) - Y(T) + H)(S - T)\sin\theta(T) \\ &\quad - K(X(S) - X(T) - K) + H(Y(S) - Y(T) + H) \\ &\approx 0 - K((S - T)\cos\theta(T) - K) \\ &\quad + H((S - T)\sin\theta(T) + H) \\ &\approx K^2(-\cos^2\theta(T) + 1) \\ &\quad + H^2(-\sin^2\theta(T) + 1) \\ &\quad + 2KH\sin\theta(T)\cos\theta(T) \\ &= (K\sin\theta(T) + H\cos\theta(T))^2. \end{aligned} \tag{A7}$$

Since θ does not vary rapidly along the layer, $\theta(S) \approx \theta(T)$, and we obtain

$$D(S) \approx \left|K\sin\theta(S) + H\cos\theta(S)\right|. \tag{A8}$$

For the solutions that we obtain, $K\sin\theta(S) + H\cos\theta(S)$ is positive, and the absolute value signs are therefore dropped.

We penalize the creation of voids by the energy

$$\begin{aligned} &P\int_{-\infty}^{\infty} (D(S) - H)_+ \, \mathrm{d}S \\ &= P\int_{-\infty}^{\infty} (K\sin\theta(S) + H\cos\theta(S) - H)_+ \, \mathrm{d}S. \end{aligned} \tag{A9}$$

Here P is the overburden pressure, and $x_+ = \max(x, 0)$. This expression represents the work done into the overburden pressure by the creation of voids between the layers. The optimal configuration is found by minimizing the potential

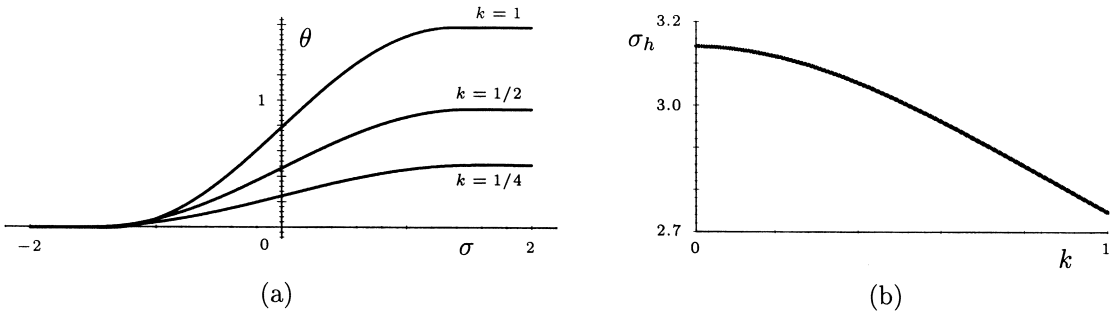

Fig. A3. Numerical calculations of the hinge profile. (a) Shows the value of θ, the layer angle, as a function of σ, the non-dimensionalized arc length. (b) Shows the length of the hinge zone as a function of k.

$$J = \frac{EI}{2}\int_{-\infty}^{\infty} \theta'(S)^2 \, \mathrm{d}S + P\int_{-\infty}^{\infty} (K \sin\theta(S) + H\cos\theta(S) - H)_+ \, \mathrm{d}S \tag{A10}$$

over all profiles θ that tend to 0 at $-\infty$ and to θ_∞ at $+\infty$. Before calculating this minimizer we non-dimensionalize S and K by H, i.e. we write $S = Hs$, $K = Hk$, and obtain

$$\begin{aligned} J &= \frac{EI}{2H}\int_{-\infty}^{\infty} \theta'(s)^2 \, \mathrm{d}s + PH^2\int_{-\infty}^{\infty} (k\sin\theta(s) + \cos\theta(s) - 1)_+ \, \mathrm{d}s \\ &= \frac{EI}{H}\left\{\frac{1}{2}\int_{-\infty}^{\infty} \theta'(s)^2 \, \mathrm{d}s + \frac{PH^3}{EI}\int_{-\infty}^{\infty} (k\sin\theta(s) + \cos\theta(s) - 1)_+ \, \mathrm{d}s\right\}. \end{aligned} \tag{A11}$$

We define the non-dimensional parameter $\lambda^2 = PH^3/EI$.

A minimizer θ of J satisfies the Euler equation

$$-\theta'' + \lambda^2(k\cos\theta - \sin\theta)\mathscr{H}(k\sin\theta + \cos\theta - 1) = 0, \tag{A12}$$

where $\mathscr{H}$ is the Heaviside function

$$\mathscr{H}(x) = \begin{cases} 1 & \text{if } x > 0 \\ 0 & \text{if } x \le 0 \end{cases}. \tag{A13}$$

The parameter λ can be scaled out of this equation by setting $\sigma = \lambda s$, so that

$$-\frac{\mathrm{d}^2\theta}{\mathrm{d}\sigma^2} + (k\cos\theta - \sin\theta)\mathscr{H}(k\sin\theta + \cos\theta - 1) = 0. \tag{A14}$$

The most important result of this modelling can be obtained without solving this equation. The fact that Eq. (A14) is independent of all material parameters implies that for all choices of these parameters the solutions are the same up to a scaling. In terms of σ, the length of the hinge region is fixed (say σ_h); therefore the hinge length of a hinge in laboratory variables is $S_\mathrm{h} = Hs_\mathrm{h} = \sigma_\mathrm{h}H/\lambda$. This equation contains the main statement of this section: at constant layer thickness the length of the hinge section is proportional to the ratio $\lambda^{-1} = \sqrt{(EI/PH^3)}$ of bending stiffness and overburden pressure. For instance, doubling the overburden pressure decreases the length of the hinge by a factor $\sqrt{2}$.

It is, however, possible to solve this equation, at least in a partially explicit way. Writing $F(\theta) = (k\sin\theta + \cos\theta - 1)_+$ and $f(\theta) = F'(\theta) = (k\cos\theta - \sin\theta)\mathscr{H}(k\sin\theta + \cos\theta - 1)$, we can multiply Eq. (A14) by θ' and integrate to obtain

$$-\frac{1}{2}\left(\frac{\mathrm{d}\theta}{\mathrm{d}\sigma}\right)^2 + F(\theta) = c, \tag{A15}$$

where c is an integration constant. Since θ, $\theta' \to 0$ as $\sigma \to -\infty$, we have $c = 0$, and therefore

$$\frac{\mathrm{d}\theta}{\mathrm{d}\sigma} = \sqrt{2F(\theta)}. \tag{A16}$$

By inverting the roles of θ and σ we can solve this equation in the form

$$\sigma = \int_{\arctan k}^{\theta(\sigma)} \frac{\mathrm{d}t}{\sqrt{2F(t)}}. \tag{A17}$$

Solution graphs are plotted in Fig. A3(a) for different values of k. This figure suggests that the length of the hinge zone—σ_h—is independent of k to first approximation. Using the formula

$$\sigma_\mathrm{h} = 2\int_0^{\arctan k} \frac{\mathrm{d}t}{\sqrt{2F(t)}} \tag{A18}$$

we plot σ_h as a function of k in Fig. A3. The fact that σ_h appears to take the value π as $k \to 0$ is no coinci-

dence; indeed if k is small, then $\sin t \sim t$, $\cos t - 1 \sim -t^2/2$, and the integral is approximated by

$$\sqrt{2}\int_0^1 \frac{d\tau}{\sqrt{\tau - \tau^2/2}}. \tag{A19}$$

Here we have substituted $k\tau$ for t. This integral has the value π, as can be verified by substituting $1 - \rho$ for τ.

References

Adhikary, D.P., Dyskin, A.V., 1997. A Cosserat continuum for layered materials. Computers and Geosciences 20, 15–45.

Adhikary, D.P., Dyskin, A.V., 1998. A continuum model of layered rock masses with non-associative joint plasticity. International Journal of Numerical Analysis and Methods in Geomechanics 22, 245–261.

Adhikary, D.P., Mühlhaus, H.-B., Dyskin, A.V., 1999. Modelling the large deformations in stratified media—the Cosserat continuum approach. Mechanics of Cohesiue–Frictional Materials 4, 195–213.

Biot, M.A., 1965. Mechanics of Incremental Deformations. Wiley, New York.

Budiansky, B., Fleck, N.A., Amazigo, J.C., 1998. On kink-band propagation in fiber composites. Journal of the Mechanics and Physics of Solids 46, 1637–1653.

Fleck, N.A., 1997. Compressive failure of fiber composites. Advances in Applied Mechanics 33, 43–117.

Fleck, N.A., Deng, L., Budiansky, B., 1995. Prediction of kink band width in compressed fiber composites. ASME Journal of Applied Mechanics 62, 329–337.

Golubitsky, M., Schaeffer, D.G., 1984. Singularities and groups in bifurcation theory. Applied Mathematical Sciences, vol. 51. Springer-Verlag, New York.

Hobbs, B.E., Means, W.D., Williams, P.F., 1976. An Outline of Structural Geology. Wiley, New York.

Hobbs, B.E., Means, W.D., Williams, P.F., 1982. The relationship between foliation and strain: an experimental investigation. Journal of Structural Geology 4, 411–428.

Hobbs, R.E., Overington, M.S., Hearle, J.W.S., Banfield, S.J., 1995. Element buckling within ropes and cables. Proceedings of Second European Conference on Flexible Pipes, Umbilicals and Marine Cables. BPP Ltd., London, pp. 7.1–7.21.

Hunt, G.W., Peletier, M.A., Champneys, A.R., Woods, P.D., Wadee, M.A., Budd, C.J., Lord, G.J., 1999. Cellular buckling in long structures. Nonlinear Dynamics 21, 3–29.

Kerr, A.D., 1964. Elastic and viscoelastic foundation models. ASME Journal of Applied Mechanics 31, 491–498.

Paterson, M.S., Weiss, L.E., 1966. Experimental deformation and folding in phylite. Geological Society of American Bulletin 77, 343–374.

Price, N.J., Cosgrove, J.W., 1990. Analysis of Geological Structures. Cambridge University Press, Cambridge.

Reid, S.R., Peng, C., 1997. Dynamic uniaxial crushing of wood. International Journal of Impact Engineering 19, 531–570.

Thompson, J.M.T., Hunt, G.W., 1973. A General Theory of Elastic Stability. Wiley, London.

Williams, P.F., Price, G.P., 1990. Origin of kinkbands and sheer-band cleavage in shear zones: an experimental study. Journal of Structural Geology 12, 145–164.

Zeeman, E.C., 1977. Catastrophe Theory: Selected papers, 1972–1977. Addison-Wesley, London.